Check for updates

Received: 5 June 2019 | Revised: 26 July 2019 | Accepted: 28 July 2019

DOI: 10.1002/aoc.5185

FULL PAPER

WILEY Applied Organometallic Chemistry

Synthesis, characterization, molecular docking studies and *in vitro* screening of new metal complexes with Schiff base as antimicrobial and antiproliferative agents

Elena Pahonțu[1] | Maria Proks[2] | Sergiu Shova[3] | Gina Lupașcu[4] | Diana-Carolina Ilieș[5] | Ștefania-Felicia Bărbuceanu[5] | Laura-Ileana Socea[5] | Mihaela Badea[6] | Virgil Păunescu[2] | Dorin Istrati[7] | Aurelian Gulea[8] | Doina Drăgănescu[9] | Cristina Elena Dinu Pîrvu[10]

[1] General and Inorganic Chemistry Department, Faculty of Pharmacy, University of Medicine and Pharmacy 'Carol Davila', 6 Traian Vuia Street, 020956 Bucharest, Romania

[2] Functional Sciences Department, Faculty of Medicine, University of Medicine and Pharmacy 'Victor Babeș', 'Pius Brinzeu', County Emergency Clinical Hospital, Oncogen Institute, 156 Liviu Rebreanu, 300723 Timișoara, Romania

[3] Institute of Macromolecular Chemistry 'Petru Poni', 41A Grigore Ghica Voda Alley, 700487 Iași, Romania

[4] Physiology Department, Faculty of Pharmacy, University of Medicine and Pharmacy 'Carol Davila', 6 Traian Vuia Street, 020956 Bucharest, Romania

[5] Organic Chemistry Department, Faculty of Pharmacy, University of Medicine and Pharmacy 'Carol Davila', 6 Traian Vuia Street, 020956 Bucharest, Romania

[6] Inorganic Chemistry Department, Faculty of Chemistry, University of Bucharest, 23 Dumbrava Rosie Street, 020462 Bucharest, Romania

[7] Department of Therapeutic Dentistry, Faculty of Dentistry 'Nicolae Testemițanu', State University of Medicine and Pharmacy, 165 Stefan cel Mare si Sfant Street, 2009 Chișinău, Moldova

[8] Laboratory of Advanced Materials in Biofarmaceuticals and Technics, Moldova State University, 60 Mateevici Street, 2009Chisinau, Moldova

[9] Pharmaceutical Physics Department, Faculty of Pharmacy, University of Medicine and Pharmacy 'Carol Davila', 6 Traian Vuia Street, 020956 Bucharest, Romania

[10] Physical and Colloidal Chemistry Department, Faculty of Pharmacy, University of Medicine and Pharmacy 'Carol Davila', 6 Traian Vuia Street, 020956 Bucharest, Romania

Correspondence

Elena Pahontu, Inorganic Chemistry Department, Faculty of Pharmacy, University of Medicine and Pharmacy 'Carol Davila', Bucharest, Romania.
Email: elenaandmihaela@yahoo.com

Maria Proks, Functional Sciences Department, Faculty of Medicine, University of Medicine and Pharmacy 'Victor Babeș', Timisoara, Romania.
Email: proks.maria@yahoo.com

Gina Lupașcu, Physiology Department, Faculty of Pharmacy, University of Medicine and Pharmacy 'Carol Davila', Bucharest, Romania.
Email: gina.lupascu@yahoo.com

A series of Cu(II), Co(II), Pd(II), Pt(II), Zn(II), Cd(II) and Fe(III) complexes were designed and synthesized using Schiff base 1-phenyl-2,3-dimethyl-4-(*N*-3-formyl-6-methylchromone)-3-pyrazolin-5-one (HL). The new metal complexes were investigated using various physicochemical techniques including elemental and thermal analyses, molar electric conductivity and magnetic susceptibility measurements, as well as spectroscopic methods. Also, the crystal structures of ligand HL and the Pd(II) complex were determined using single-crystal X-ray diffraction analysis. For all compounds, the antimicrobial activity was studied against a series of standard strains: *Staphylococcus aureus*, *Bacillus cereus*, *Enterococcus faecalis*, *Escherichia coli*, *Acinetobacter baumannii*, *Candida albicans*, *Candida krusei* and *Cryptococcus neoformans*. The *in vitro* antiproliferative activity of the ligand and complexes was evaluated against ten cancer cell lines: MSC, A375, B16 4A5, HT-29, MCF-

This is an open access article under the terms of the Creative Commons Attribution License, which permits use, distribution and reproduction in any medium, provided the original work is properly cited.
© 2019 The Authors. *Applied Organometallic Chemistry* published by John Wiley & Sons, Ltd.

7, HEp-2, BxPC-3, RD, MDCK and L20B. At 10 μM concentration a significant cytotoxic effect of the Co(II), Pd(II) and Cd(II) complexes was observed against B16 4A5 murine melanoma cells. The Zn(II) complex is active against HEp-2, RD and MDCK cancer cell lines, where IC_{50} values vary between 1.0 and 77.6 and for BxPC-3 the activity index versus doxorubicin is 3.7 times higher.

KEYWORDS

antimicrobial activity, antiproliferative activity, metal complexes, molecular docking, Schiff base

1 | INTRODUCTION

Schiff bases represent an important class of organic compounds and have received much attention in coordination and biological chemistry.[1,2] Schiff bases are one of the most powerful group of chelators due high electron density on azomethine nitrogen atom. The chelation of Schiff bases with transition metal ions has been observed to improve the biological potentials of such bases, and therefore metal complexes of various Schiff bases are well known as antioxidant, antibacterial, antifungal, anticancer, antitubercular and anti-inflammatory agents.[3–10]

Antipyrine (N-heterocyclic compound) and its derivatives exhibit a wide range of biological activities like analgesic, antibacterial, antifungal, anti-inflammatory, antiviral, antiarrhythmic, antipyretic and antioxidant activities.[11–19] Also, chromone derivatives, compounds with aromatic planar structure, have been of special interest in organic synthesis due to their biological activities such as anticonvulsant, antioxidant, antibacterial, antifungal, anticancer, anti-HIV, antiulcer and anti-inflammatory activities.[20–25]

This paper is a continuation of our previous research and it presents the synthesis and characterization of new copper(II), cobalt(II), palladium(II), platinum(II), zinc(II), cadmium(II) and iron(III) complexes with Schiff base derived from 4-amino-2,3-dimethyl-1-phenyl-3-pyrazolin-5-one and 3-formyl-6-methylchromone. In addition, the antimicrobial activity of the metal complexes was evaluated using the paper disc diffusion method[26] (for qualitative determination) and the serial dilutions in liquid broth method[27] (for determination of minimum inhibitory concentration). The antiproliferative activity of the complexes was investigated against various cancer cell lines: MSC, A375, B16 4A5, HT-29, MCF-7, HEp-2, BxPC-3, RD, MDCK and L20B. Finally, molecular docking analysis was also performed to elucidate the mode of action of these compounds, to support the effective binding of molecules at the active site of protein.[28–31]

2 | EXPERIMENTAL

2.1 | Materials

4-Amino-2,3-dimethyl-1-phenyl-3-pyrazolin-5-one and 3-formyl-6-methylchromone (Sigma-Aldrich, Munich, Germany) were used as received. $CuBr_2$, $CoCl_2{\cdot}6H_2O$, $Pd(CH_3COO)_2$, $K_2[PtCl_4]$, $ZnCl_2$, $CdCl_2{\cdot}2.5H_2O$ and $FeCl_3{\cdot}6H_2O$ (Merck, Darmstadt, Germany) were used as supplied. Solvents used for the reactions were purified and dried by conventional methods.[32]

2.2 | Synthesis of Schiff base 1-phenyl-2,3-dimethyl-4-(*N*-3-formyl-6-methylchromone)-3-pyrazolin-5-one (HL)

The Schiff base HL was synthesized by refluxing equimolar amounts of 4-amino-2,3-dimethyl-1-phenyl-3-pyrazolin-5-one and 2-hydroxy-4-methoxybenzaldehyde in ethanol according to a previously reported experimental protocol.[33]

IR (KBr, cm^{-1}): υ(C═O) 1655; υ(C═N) 1619; υ(Ar—OH) 1137; υ(Ar—O—$C_{aliphatic}$) 1236. The ^{1}H NMR spectrum ($CDCl_3$; δ, ppm; *J*, Hz), recorded in $CDCl_3$, of HL has the following signals confirming the structure of the ligand: δ = 1.03 (t, *J* = 7.1, 3H, CH_3, H—C5); 2.30 (s, 6H, H_3C—C6 and H_3C—C18); 3.05 (s, 3H, N—CH_3, N-3); 3.62 (q, *J* = 7.1, 2H, OCH_2, C-7); 5.83 (s, 1H, H—C4); 6.92 (d, *J* = 8.3,1H, H-13); 7.29 (dd, *J* = 8.3, 2.2, 1H, H-12); 7.32 (d, *J* = 7.4, 2H, H-20 and H-24); 7.52 (m, 3H, H-21, H-22, H-23); 7.90 (s, 1H, H-3); 9.24 (s, 1H, —CH═N—). ^{13}C NMR spectrum (DMSO-d_6, δ, ppm): 10.13 (CH_3—C14); 15.11 (C-5); 20.33 (CH_3—C10); 36.00(CH_3—N); 62.83 (C-5); 99.88 (C-4); 102.39 (Cq); 117.75 (C-13); 122.44(Cq); 124.24 (CH20,24); 125.38 CH); 127.07 (CH); 129.33 (CH21,23); 130.77 (Cq); 134.88 (CH); 145.19 (Cq); 148.81 (CH);153.40 (Cq); 159.61 (Cq); 179.76 (C-4).

10990739, 2019, 11, Downloaded from https://onlinelibrary.wiley.com/doi/10.1002/aoc.5185 by Republic of Moldova Hinari NPL, Wiley Online Library on [18/09/2023]. See the Terms and Conditions (https://onlinelibrary.wiley.com/terms-and-conditions) on Wiley Online Library for rules of use; OA articles are governed by the applicable Creative Commons License

2.3 | General procedure for preparation of metal complexes

The metal complexes were prepared by the direct reaction between the ligand and the corresponding metal salts.

2.3.1 | Synthesis of complex [CuL(Br)]·H_2O (1)

An methanol solution (10 ml) of $CuBr_2$ (0.223 g, 1 mmol) was added dropwise to a stirred methanol solution (20 ml) of HL (0.435 g, 1 mmol) and 1–2 drops of triethylamine (Et_3N). The resulting solution was stirred for 6 h at 50°C. After a few days, the brown-coloured solid was filtered, washed with hot water, then methanol followed by ether and dried *in vacuo*.

Yield 76%; m.p. >300°C; molecular weight: 565.5. Anal. Calcd for $C_{23}H_{24}CuN_3O_5Br$ (%): C, 48.80; H, 4.24; N, 7.42; Cu, 11.22. Found (%): C, 48.93; H, 4.18; N, 7.24; Cu, 11.05. Selected IR peaks (KBr, cm^{-1}): υ(C═O) 1641; υ(C═N) 1608; υ(Ar—OH) 1122; υ(Ar—O—$C_{aliphatic}$) 1236.

2.3.2 | Synthesis of complex [CoL_2] (2)

Complex **2** was prepared similarly, using $CoCl_2·6H_2O$ and ligand HL at a molar ratio M:L of 1:2. The mixture was stirred at 50°C for 4 h. The brown-coloured solid was filtered, washed with hot water, then ethanol followed by ether and dried *in vacuo*.

Yield: 80%; m.p. >300°C; molecular weight: 867. Anal. Calcd for $C_{46}H_{44}CoN_6O_8$ (%): C, 63.66; H, 5.07; N, 9.68. Found (%): C, 63.90; H, 4.88; N, 9.43. Selected IR peaks (KBr, cm^{-1}): υ(C═O) 1630; υ(C═N) 1609; υ(Ar—OH) 1126; υ(Ar—O—$C_{aliphatic}$) 1236.

2.3.3 | Synthesis of complex [PdL_2]·1.25H_2O (3)

Complex **3** was prepared similarly, using $Pd(CH_3COO)_2$ at a molar ratio M:L of 1:1. The product was a brown-reddish solid.

Yield: 77%; m.p. >300°C; molecular weight: 935.77. Anal. Calcd for $C_{46}H_{44.5}Pd\ N_6O_{9.25}$ (%): C, 58.98; H, 4.75; N, 8.97; Pd, 11.37. Found (%): C, 59.21; H, 4.67; N, 8.74; Pd, 11.28. Selected IR peaks (KBr, cm^{-1}): υ(C═O) 1654; υ(C═N) 1602; υ(Ar—OH) 1124; υ-(Ar—O—$C_{aliphatic}$) 1239.

2.3.4 | Synthesis of complex [PtLCl]·H_2O (4)

Complex **4** was synthesized by stirring a hot solution of HL (0.435 g, 1 mmol) in methanol (20 ml) with $K_2[PtCl_4]$ (0.415, 1 mmol) dissolved in 10 ml of distilled water–methanol solution (1:2, v/v). The mixture was refluxed for 4 h. The brown precipitate was filtered, washed with hot water and methanol followed by ether and dried *in vacuo*.

Yield: 82%; m.p. >300°C; molecular weight: 652.5. Anal. Calcd for $C_{23}H_{24}PtN_3O_5Cl$ (%): C, 42.29; H, 3.67; N, 6.43. Found (%): C, 42.53; H, 3.29; N, 6.14. Selected IR peaks (KBr, cm^{-1}): υ(C═O) 1635; υ(C═N) 1605; υ(Ar—OH) 1127; υ-(Ar—O—$C_{aliphatic}$) 1235.

2.3.5 | Synthesis of complex [ZnLCl] (5)

A chloroform solution (15 ml) of HL (0.435 g, 1 mmol) was added to $ZnCl_2$ (0.136 g, 1 mmol) dissolved in 15 ml of distilled water–ethanol solution (1:2, v/v). The resulting solution was refluxed for 6 h. The yellow-coloured solid was filtered, washed with hot water, ethanol and ether and then dried *in vacuo*.

Yield: 72%; m.p. >300°C; molecular weight: 504.9. Anal. Calcd for $C_{23}H_{22}ZnN_3O_4Cl$ (%): C, 54.66; H, 4.35; N, 8.31. Found (%): C, 54.89; H, 4.27; N, 8.10. Selected IR peaks (KBr, cm^{-1}): υ(C═O) 1638; υ(C═N) 1602; υ(Ar—OH) 1126; υ(Ar—O—$C_{aliphatic}$) 1239.

2.3.6 | Synthesis of complex [CdLCl]·2H_2O (6)

To a stirred solution of $CdCl_2·2.5H_2O$ (0.228 g, 1 mmol) in methanol (10 ml) was added a solution of ligand HL (0.435 g, 1 mmol) in chloroform (15 ml). The mixture was stirred at reflux temperature for 8 h to afford a yellow solid.

Yield: 75%; m.p. >300°C; molecular weight: 587.91. Anal. Calcd for $C_{23}H_{26}CdN_3O_6Cl$ (%): C, 46.94; H, 4.42; N, 7.14. Found (%): C, 47.15; H, 4.36; N, 6.87. Selected IR peaks (KBr, cm^{-1}): υ(C═O) 1641; υ(C═N) 1606; υ(Ar—OH) 1122; υ(Ar—O—$C_{aliphatic}$) 1237.

2.3.7 | Synthesis of complex [$FeL_2(H_2O)_2$]Cl (7)

To a solution of HL (0.435 g, 1 mmol) in methanol (20 ml) was added a solution of $FeCl_3·6H_2O$ (0.270 g, 1 mmol) in methanol (10 ml). The mixture was refluxed for 4 h. After a few days, the brown-coloured solid was

10990739, 2019, 11, Downloaded from https://onlinelibrary.wiley.com/doi/10.1002/aoc.5185 by Republic of Moldova Hinari NPL, Wiley Online Library on [18/09/2023]. See the Terms and Conditions (https://onlinelibrary.wiley.com/terms-and-conditions) on Wiley Online Library for rules of use; OA articles are governed by the applicable Creative Commons License

filtered, washed with hot water, then methanol followed by ether and dried in *vacuo*.

Yield: 74%; m.p. >300°C; molecular weight: 935.35. Anal. Calcd for $C_{46}H_{48}FeN_6O_{10}Cl$ (%): C, 59.01; H, 5.13; N, 8.98. Found (%): C, 59.32; H, 5.03; N, 8.74. Selected IR peaks (KBr, cm^{-1}): υ(C═O) 1653; υ(C═N) 1608; υ(Ar—OH) 1123; υ(Ar—O—$C_{aliphatic}$) 1236.

2.4 | Physical measurements

The chemical elemental analysis for the determination of C, H, N was done with a Carlo-Erba LA-118 microdosimeter. The Cu(II) content was determined using atomic absorption spectroscopy with a Carl Zeiss Jena AAS 1N spectrometer; palladium was determined following the method described by Fries and Getrost.[34] IR spectra were recorded with a Specord-M80 spectrophotometer in the range 400–4000 cm^{-1} using KBr pellets. ^1H NMR and ^{13}C NMR spectra were recorded at room temperature with a Bruker DRX 400 spectrometer (Billerica, MA, USA) in deuterated dimethylsulfoxide (DMSO-d_6), using tetramethylsiloxane as the internal standard. Electronic spectra were recorded using a JascoV-670 spectrophotometer (Tokyo, Japan), in diffuse reflectance, using MgO dilution matrices. Magnetic susceptibility measurements were done at room temperature in the polycrystalline state with a Faraday magnetic balance (homemade). Fast atom bombardment (FAB) mass spectra were recorded with a JMS-AX-500 mass spectrometer (Tokyo, Japan). Gas chromatography–mass spectrometry analysis was performed with a GCMS-QP5050A instrument (Shimadzu, Duisburg, Germany). The molar conductance of the complexes in dimethylformamide (DMF) solutions (10^{-3} M), at room temperature, were measured using a Consort C-533 conductivity instrument. The complexes were studied using thermogravimetry in a static air atmosphere, with a sample heating rate of 10°C min^{-1} using an STA 6000 (PerkinElmer, Waltham, MA, USA).

2.5 | X-ray crystallography

X-ray diffraction measurements were carried out with an Oxford-Diffraction XCALIBUR E CCD diffractometer equipped with graphite-monochromated Mo Kα radiation. A single crystal was positioned at 40 mm from the detector and 251 frames were measured each for 110 s over a 1° scan width. Unit cell determination and data integration were carried out using the CrysAlis package of Oxford.[35] The structure was solved by direct methods using Olex2[36] software with the SHELXT structure solution program and refined by full-matrix least-squares on F^2 with SHELXL-2015.[37] Hydrogen atoms attached to carbon were placed in fixed, idealized positions and refined as rigidly bonded to the corresponding non-hydrogen atoms. Positional parameters of the hydrogen atoms attached to oxygen atoms were obtained from difference Fourier syntheses and verified by the hydrogen bond parameters. The positional parameters of disordered fragments of the ligand were refined using available tools (PART, DFIX and SADI) of SHELXL-2015 and a combined anisotropic/isotropic refinement was applied for non-hydrogen atoms. Molecular plots were obtained using the Olex2 program. The crystallographic data and refinement details are presented in Table 1, while bond lengths and angles are summarized in Table 2.

2.6 | Biological studies

2.6.1 | Antibacterial and antifungal activities

The antibacterial activity of the complexes was determined under liquid nutritive environment (2% of peptonate bullion; pH 7.0) using the successive dilutions method. *Staphylococcus aureus* ATCC 25923, *Bacillus cereus* ATCC 11778, *Enterococcus faecalis* ATCC 19433, *Escherichia coli* ATCC 25922 and *Acinetobacter baumannii* ATCC BAA-747 standard stems were used as reference cultures for *in vitro* experiments. The dissolution of studied substances in DMF, microorganisms, cultivation, obtaining of suspensions, determination of minimal inhibitory concentration (MIC) and determination of minimal bactericidal concentration (MBC) were carried out according to a previous report.[27]

Antimycotic properties of the synthesized substances were investigated *in vitro* using laboratory stems of *Candida albicans* ATCC 10231, *Candida krusei* ATCC 6258 and *Cryptococcus neoformans*. The activity was determined in liquid Sabouroud nutritive environment (pH 6.8). The inoculates were prepared from fungi stems which were harvested during 3–7 days. Their concentration in suspension was (2–4) × 10^6 colony forming units per millilitre. Cultures for levures and micelles were incubated at 37°C during 7 and 14 days, respectively.

2.6.2 | Antiproliferative activity

Preparation of test substance solutions

The eight test substances (ligand HL and its metal complexes) were dissolved in DMSO (Sigma-Aldrich, Ayrshire, UK) in order to obtain 5 μM stock solutions. The solutions were stored at 2–8°C.

10990739, 2019, 11, Downloaded from https://onlinelibrary.wiley.com/doi/10.1002/aoc.5185 by Republic of Moldova Hinari NPL, Wiley Online Library on [18/09/2023]. See the Terms and Conditions (https://onlinelibrary.wiley.com/terms-and-conditions) on Wiley Online Library for rules of use; OA articles are governed by the applicable Creative Commons License

TABLE 1 Crystal data and structure refinement parameters for complex **3**

Empirical formula	$C_{46}H_{44.5}Pd\ N_6O_{9.25}$
Formula weight	935.77
Temperature (K)	160
Space group	$P2_1/c$
a (Å)	13.1955(17)
b (Å)	7.9426(8)
c (Å)	20.926(3)
α (°)	90
β (°)	90.802(11)
γ (°)	90
V (Å^3)	2193.0(4)
Z	2
ρ_{calcd} (g cm^{-3})	1.417
μ (mm^{-1})	0.487
Crystal size (mm)	0.25 × 0.20 × 0.02
2θ range (°)	3.894 to 48.814
Reflections collected	9185
Independent reflections	3598 [R_{int} = 0.0918]
Data/restraints/parameters	3598/43/336
R_1[a]	0.0779
wR_2[b]	0.1623
GOF[c]	1.046
	1.03/−0.70

[a]$R_1 = \Sigma||F_o| - |F_c||/\Sigma|F_o|$.

[b]$wR_2 = \{\Sigma[w(F_o^2 - F_c^2)^2]/\Sigma[w(F_o^2)^2]\}^{1/2}$.

[c]GOF = $\{\Sigma[w(F_o^2 - F_c^2)^2]/(n-p)\}^{1/2}$, where n is the number of reflections and p is the total number of parameters refined.

TABLE 2 Bond lengths and angles for compound **3**

Bonds lengths (Å)			
C1–C2	1.477(9)	C14–N2	1.386(8)
C1–C11	1.399(9)	C14–O3	1.248(8)
C1–O1	1.280(8)	C15–C16	1.484(9)
C2–C3	1.394(10)	C15–N3	1.366(8)
C2–C8	1.375(10)	C17–N3	1.481(8)
C3–C4	1.396(10)	C18–C19	1.360(11)
C4–C5	1.495(10)	C18–C23	1.389(11)
C4–C6	1.379(11)	C18–N2	1.420(9)
C6–C7	1.363(12)	C19–C20	1.387(13)
C7–C8	1.384(11)	C20–C21	1.339(14)
C8–O2	1.382(8)	C21–C22	1.350(13)
C11–C12	1.418(10)	C22–C23	1.382(12)
C11–C9	1.464(15)	N1–Pd1	1.989(5)
C12–N1	1.295(8)	N2–N3	1.404(7)
C13–C14	1.441(9)	O1–Pd1	1.986(5)
C13–C15	1.348(9)	O2–C9	1.409(16)
C13–N1	1.436(8)	C9–O4	1.444(11)
Angles (°)			
C11–C1–C2	116.3(7)	N3–C15–C16	120.3(6)
O1–C1–C2	116.9(7)	C19–C18–C23	119.5(8)
O1–C1–C11	126.6(7)	C19–C18–N2	119.0(8)
C3–C2–C1	121.6(7)	C23–C18–N2	121.5(7)
C8–C2–C1	119.7(7)	C18–C19–C20	119.7(10)
C8–C2–C3	118.4(8)	C21–C20–C19	120.2(10)
C2–C3–C4	121.7(8)	C20–C21–C22	121.3(10)
C3–C4–C5	121.4(8)	C21–C22–C23	119.7(10)
C6–C4–C3	116.5(8)	C22–C23–C18	119.5(9)
C6–C4–C5	122.0(8)	C12–N1–C13	114.5(6)
C7–C6–C4	123.9(8)	C12–N1–Pd1	121.4(5)
C6–C7–C8	118.0(8)	C13–N1–Pd1	124.0(4)
C2–C8–C7	121.5(8)	C14–N2–C18	126.6(6)
C2–C8–O2	122.7(7)	C14–N2–N3	109.4(5)
O2–C8–C7	115.7(8)	N3–N2–C18	117.8(6)
C1–C11–C12	122.2(7)	C15–N3–C17	119.4(6)
C1–C11–C9	120.3(8)	C15–N3–N2	106.2(5)
C12–C11–C9	117.0(8)	N2–N3–C17	114.0(6)
N1–C12–C11	126.9(7)	C1–O1–Pd1	123.2(5)
C15–C13–C14	107.7(6)	C8–O2–C9	118.0(7)
C15–C13–N1	127.1(6)	O1–Pd1–N1[1]	88.5(2)
N1–C13–C14	125.2(6)	O1–Pd1–N1	91.5(2)

(Continues)

Each stock solution was formulated in various concentrations (1, 2.5, 5, 7.5, 10 or 100 μM) to obtain the half maximal inhibitory concentration (IC_{50}) values, as follows. By successive dilution of the stock solutions with the specific culture medium for each cell line, five final solutions covering a concentration range between 1 and 10 μM for all complexes were obtained.

Cell culture

Each cell line was cultured in specific growth medium as follows. Mesenchymal stem cells (MSC) were isolated from tissue infrapatelar Hoffa and were cultured in alpha-MEM (minimum essential medium, Sigma-Aldrich, Bucharest, Romania) supplemented with 10% foetal calf serum (FCS; PromoCell, Heidelberg, Germany), 10 ng ml^{-1} fibroblast growth factor (Sigma, St Louis, MO, USA), 1% mixture of penicillin–streptomycin

10990739, 2019, 11, Downloaded from https://onlinelibrary.wiley.com/doi/10.1002/aoc.5185 by Republic of Moldova Hinari NPL, Wiley Online Library on [18/09/2023]. See the Terms and Conditions (https://onlinelibrary.wiley.com/terms-and-conditions) on Wiley Online Library for rules of use; OA articles are governed by the applicable Creative Commons License

TABLE 2 (Continued)

Angles (°)			
N2–C14–C13	105.2(6)	O2–C9–C11	115.8(9)
O3–C14–C13	130.8(7)	O2–C9–O4	106.1(10)
O3–C14–N2	124.0(6)	O4–C9–C11	104.8(10)
C13–C15–C16	128.8(7)	C9–O4–C10	123.9(16)
C13–C15–N3	110.8(6)		

Symmetry code: $^{1}2 - x, 2 - y, 1 - z$.

(Pen/Strep; 10 000 IU ml^{-1}; PromoCell) and 1% glutamine (PromoCell).

A375 human melanoma cells (ATCC, Manassas, VA, USA) and B16 4A5 murine melanoma cells (ATCC) were cultured in Dulbecco's modified Eagle's medium supplemented with 10% FCS (PromoCell) and 1% mixture of Pen/Strep (10 000 IU ml^{-1}; PromoCell).

HT-29 colon carcinoma cells (ATCC) and MCF-7 breast cancer cells were cultured in RPMI 1640 (Roswell Park Memorial Institute) medium supplemented with 10% FCS (PromoCell) and 1% mixture of Pen/Strep (10 000 IU ml^{-1}; PromoCell). The cells were incubated at 37°C in a humidified atmosphere containing 5% CO_2 until they became almost confluent.

Also, epithelial cancer cells of line HEp-2, human pancreatic adenocarcinoma cells of line BxPC-3, human muscle rhabdomyosarcoma spindle and large multinucleated cells of line RD, Madin Darby canine kidney epithelial normal cells of line MDCK and a mouse cell line genetically engineered to express the human poliovirus receptor (L20B) were used in this study. BxPC-3 and HEp-2 lines were cultured as monolayers in RPMI 1640 medium containing L-glutamine (2 nM), antibiotics Pen/Strep (final concentration 100 IU ml^{-1} penicillin and 100 μg ml^{-1} streptomycin) and supplemented with foetal bovine serum (FBS; 10% v/v).

Cell lines RD and MDCK were cultured in Dulbecco's modified essential medium with L-glutamine (4 mM), glucose (4.5 g l^{-1}), bovine albumin fraction (0,2% v/v), HEPES buffer (*N*-2-hydroxyethylpiperazine-*N*′-2-ethanesulfonic acid) (20 mM), antibiotics Pen/Strep (final concentration 100 U ml^{-1} penicillin and 100 μg ml^{-1} streptomycin) and supplemented with FBS (10% v/v). Cells were maintained at 37°C in a 2–5% humidified CO_2 atmosphere in an incubator in 75 cm^2 culture dishes, and used for experiments between passages 5 and 16. The compounds were dissolved at the time of the experiments.

Cell viability assay: Alamar blue *in vitro* analysis

All tested cell lines were seeded in 96-well microplates (10 000 cells per well) and allowed to adhere overnight. After 24 h the cells were treated with the final prepared substance solutions/fresh medium containing the test compounds (100 μl per well) in quadruplicate and were incubated for again for 24 h. Finally after the incubation time, 10 μl of Alamar blue solution (Invitrogen, USA) was added to each well and the cells were incubated at 37°C for 4 h (A375, B16 4A5, HT-29 and MCF-7 cell lines) or for 8 h (MSC cell line).

The samples were analysed using a spectrophotometric plate reader (Infinite M 200 PRO, TECAN, Austria) at 570 and 600 nm and cell viability was determined. All measurements were performed in quadruplicate. Untreated cells were used as controls. Concentrations between 1 and 10 μM were used in order to establish the IC_{50} values for all test substances. The IC_{50} values were calculated using the formula

$$IC_{50} = \frac{(\varepsilon_{ox})\lambda_2 A\lambda_1 - (\varepsilon_{ox})\lambda_1 A\lambda_2 \text{ of test agent dilution}}{(\varepsilon_{ox})\lambda_2 A°\lambda_1 - (\varepsilon_{ox})\lambda_1 A°\lambda_2 \text{ of untreated positive growth control}} \times 100$$

where ε_{ox} = molar extinction coefficient of Alamar blue oxidized form (blue); A = absorbance of test wells; $A°$ = absorbance of positive growth control well (cells without tested compounds); λ_1 = 570 nm; and λ_2 = 600 nm. The results are presented as mean value ± standard deviation.

One way ANOVA was used to determine the statistical difference between all the experiments; *, ** and *** indicate $p < 0.05$, $p < 0.01$ and $p < 0.001$, respectively.

Cell proliferation: resazurin assay

Cells of lines HEp-2, BxPC-3, RD, MDCK and L20B were trypsinized with trypsin–EDTA (0.05%; Invitrogen) and counted under an inverted microscope (Olympus). The cell proliferation assay was performed using resazurin (7-hydroxy-3*H*-phenoxazin-3-one-10-oxide sodium salt) (Sigma), which allowed us to measure the number of viable cells.

In brief, plate out, in triplicate of 1×10^4 cells in a total of 100 μl of medium in 96-well microtiter plates (Becton Dickinson and Company, Lincoln Park, NJ, USA) were

10990739, 2019, 11, Downloaded from https://onlinelibrary.wiley.com/doi/10.1002/aoc.5185 by Republic of Moldova Hinari NPL, Wiley Online Library on [18/09/2023]. See the Terms and Conditions (https://onlinelibrary.wiley.com/terms-and-conditions) on Wiley Online Library for rules of use; OA articles are governed by the applicable Creative Commons License

incubated at 37°C, 2% CO_2. Compounds were dissolved in DMSO to prepare the stock solution of 10 mM. These compounds and doxorubicin (DOX) were diluted at multiple concentrations with culture media, added to each well and incubated for 24 h. Following each treatment, 20 μl of resazurin indicator solution was added to each well and incubated for 4 h. Subsequently, the absorbance was read using 570 and 600 nm filters. The measurement was made with an imaging hybrid reader (Synergy H1, Biotek).

The percentage inhibition was calculated according to the formula

$$100 - \frac{\text{Abs } 570\,\text{nm}_{\text{sample}} - \text{Abs } 600\,\text{nm}_{\text{sample}}}{\text{Abs } 570\,\text{nm}_{\text{control}} - \text{Abs } 600\,\text{nm}_{\text{control}}} \times 100$$

The IC_{50} values were evaluated using statistical software.

Cell proliferation: MTS assay

The cell proliferation assay was performed using 3-(4,5-dimethylthiazol-2-yl)-5-(3-carboxymethoxyphenyl)-2-(4-sulfophenyl)-2*H*-tetrazolium (MTS; Cell Titer 96 Aqueous, Promega, USA), which allowed us to measure the number of viable HL-60 cells. In brief, triplicate cultures of 1×10^4 cells in a total of 100 μl of medium in 96-well microtiter plates (Becton Dickinson and Company) were incubated at 37°C, 5% CO_2. Compounds were dissolved in ethanol to prepare stock solutions of 1×10^{-2} M. These compounds and DOX (Novapharm, Toronto, Canada) was diluted at multiple concentrations with culture media, added to each well and incubated for 3 days. Following each treatment, 20 μl of MTS was added to each well and incubated for 4 h. MTS is converted to water-soluble coloured formazan by a dehydrogenase enzyme present in metabolically active cells. Subsequently, the plates were read at 490 nm using a microplate reader (Molecular Devices, Sunnyvale, CA).

2.7 | Molecular docking

In order to understand better the effectiveness of the ligand and complexes, molecular docking was performed. The software used to predict the binding affinity of compounds was AutoDock 4.2.[38] For molecular docking calculations, the crystal structures of enzymes were downloaded from the Royal Collaboratory for Structural Bioinformatics, RCSB Protein Data Bank (http://www.rcsb.org/pdb/).[39] Water molecules and co-crystallized ligands were removed from the .pdb. The structure of the Zn complex was drawn and optimized using Avogadro 1.2.0.[40] In order to perform molecular docking for the ligand and the Pd complex, their crystal structures were used. Preparation of the compounds and proteins, polar hydrogen atoms and partial charges (Kollman and Gasteiger charges) were performed using AutoDock Tools 1.5.6[38] that saved them as pdbqt. AutoDock Vina 1.1.2[41] was the software used to perform molecular docking. It is based on algorithms that, by setting the grid box, are able to predict compound poses within the protein target and to asses them by scoring functions. The spacing dimensions of the grid were of 1 Å. The three-dimensional results of the interactions between the target and compound were analysed and illustrated with PyMOL software.[42]

3 | RESULTS AND DISCUSSION

The Schiff base HL was synthesized by refluxing equimolar amounts of 3-formyl-6-methylchromone and 4-amino-

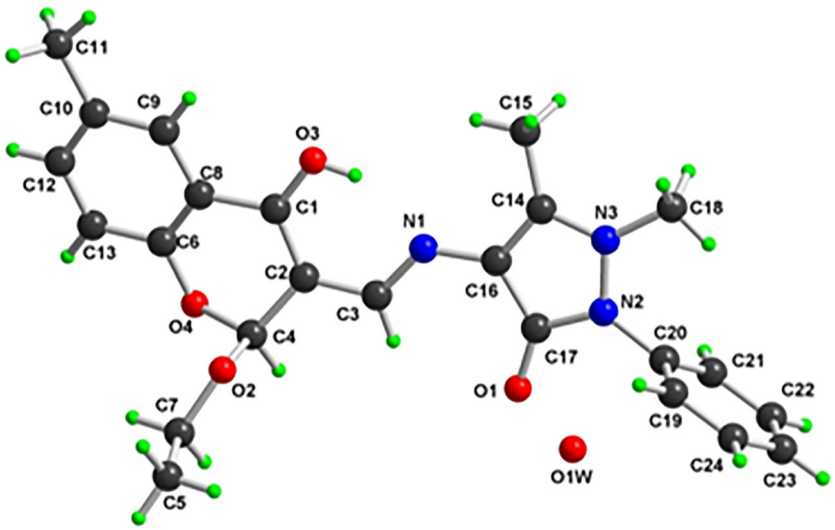


FIGURE 1 X-ray structure of Schiff base HL

10990739, 2019, 11, Downloaded from https://onlinelibrary.wiley.com/doi/10.1002/aoc.5185 by Republic of Moldova Hinari NBL, Wiley Online Library on [18/09/2023]. See the Terms and Conditions (https://onlinelibrary.wiley.com/terms-and-conditions) on Wiley Online Library for rules of use; OA articles are governed by the applicable Creative Commons License

2,3-dimethyl-1-phenyl-3-pyrazolin-5-one in ethanol according to a previously described experimental protocol.[33] The structure of the ligand was established using IR, ^{1}H NMR, ^{13}C NMR, UV–visible and mass spectroscopies and X-ray diffraction analysis (Figure 1, Table S1).

All complexes were prepared by the direct reaction between HL and the corresponding metal salts. The complex of HL with the cobalt salt was synthesized in 1:2 molar ratio, [Co:HL], but copper, palladium, platinum, zinc, cadmium and iron coordination compounds were synthesized similarly, but in 1:1 molar ratio, [M:HL].

The metal complexes are microcrystalline solids that are stable in air and decompose at temperatures greater than 250°C. They are insoluble in organic solvents such as chloroform, acetone, methanol and ethanol, but soluble in DMF and DMSO. The molar conductivity values (20–43 Ω^{-1} cm^2 mol^{-1}) of complexes **1**–**6** in 10^{-3} M DMF solution show that they are non-electrolytes; complex **7** (84 Ω^{-1} cm^2 mol^{-1}) is an electrolyte.[43]

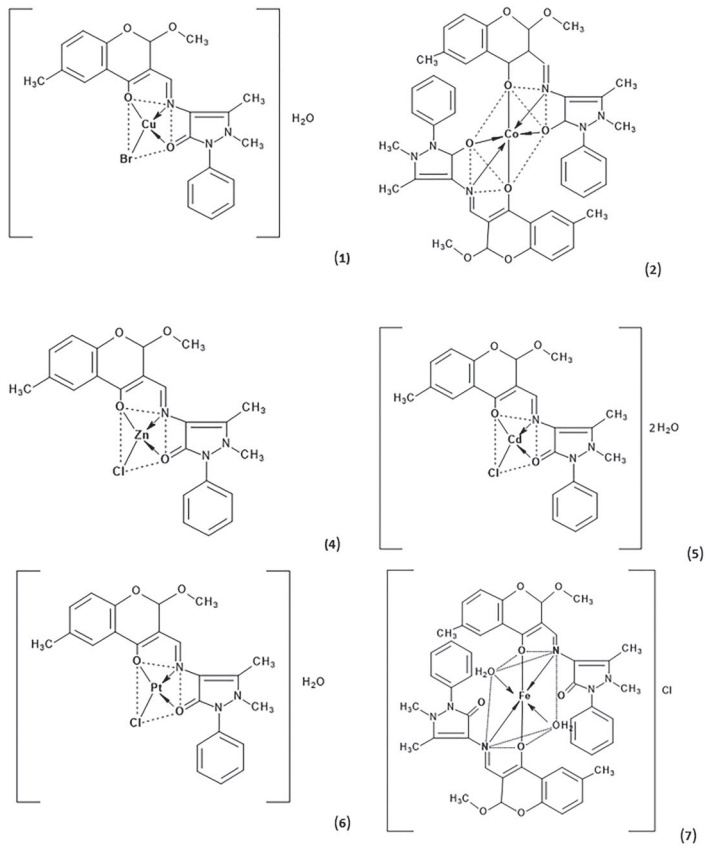
The proposed molecular formulas for complexes **1**–**7** (Scheme 1) are in agreement with the stoichiometries obtained based on analytical data (see Section 2).

3.1 | Structural characterization of complex 3

According to X-ray crystallographic analysis, compound **3** crystallizes in $P2_1/c$ space group of monoclinic system. It has a molecular crystal structure which comprises [PdL_2] neutral entities and H_2O as co-crystallized molecules in 1:1.25 stoichiometric ratio. The result of X-ray diffraction investigation is shown in Figure 2. The Pd atom, which sites on the inversion centre, exhibits a square-planar N_2O_2 coordination environment provided by two bidentate mono-deprotonated ligands L^- at Pd1–N1 1.989(5) and Pd1–O1 1.986(5) Å distances, respectively. The analysis of the crystal structure revealed the formation of a two-dimensional architecture formed due to C═H···O hydrogen bonding. A view of a two-dimensional supramolecular layer is shown in Figure 3. The main crystal structure motif is characterized as parallel packing of discrete two-dimensional layers (Figure 4). This results in the formation of relatively large areas as rectangular channels along the *b* direction filled with disordered solvent water molecules.

3.2 | IR spectra

The characteristic IR bands for the free ligand are different from those for the related complexes, which provide



SCHEME 1 Proposed structures of the metal complexes **1**, **2**, **4**–**7**

10990739, 2019, 11, Downloaded from https://onlinelibrary.wiley.com/doi/10.1002/aoc.5185 by Republic of Moldova Hinari NPL, Wiley Online Library on [18/09/2023]. See the Terms and Conditions (https://onlinelibrary.wiley.com/terms-and-conditions) on Wiley Online Library for rules of use; OA articles are governed by the applicable Creative Commons License

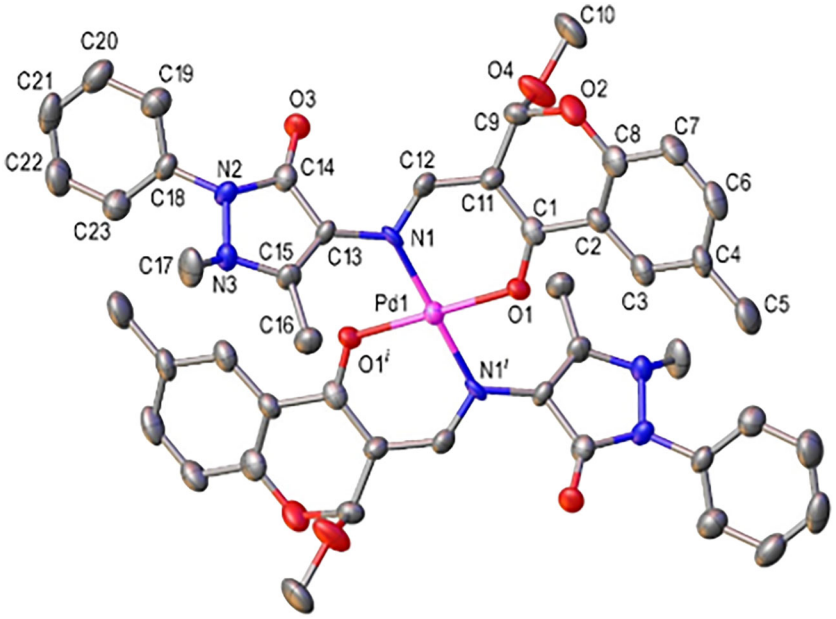


FIGURE 2 X-ray molecular structure of $[PdL_2]$ complex with atom labelling and thermal ellipsoids at 40% probability level. Hydrogen atoms are not shown

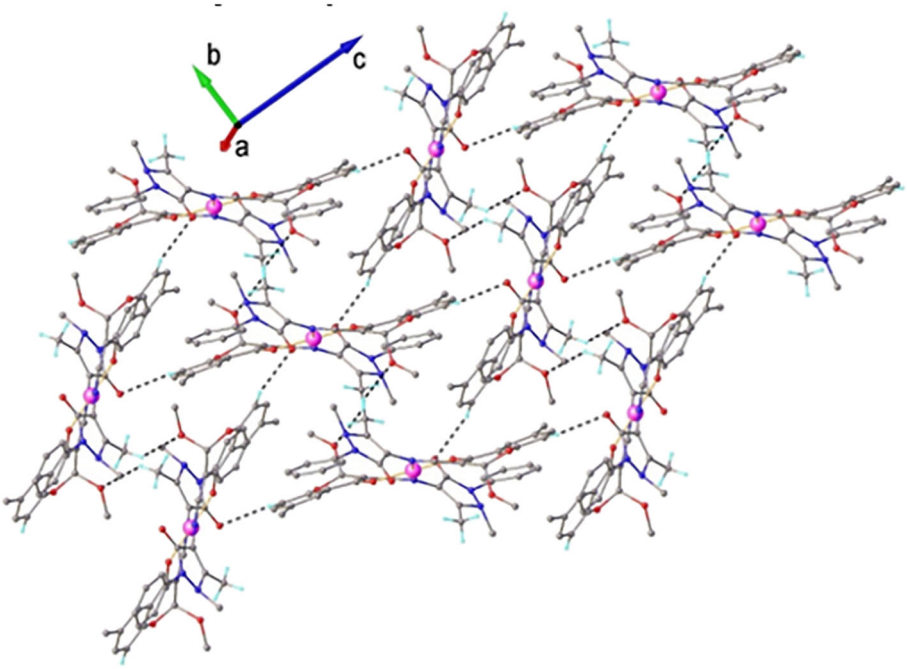


FIGURE 3 Two-dimensional supramolecular layer in the crystal structure of **3** viewed along *a*-axis

significant indications regarding the bonding sites of the Schiff base ligand.

The IR spectrum of the free Schiff base showed a strong absorption at 1619 cm^{-1} due to the azomethine υ(C═N) group. This absorption is shifted by 10–17 cm^{-1} to lower frequency in the spectra of the complexes indicating coordination via the azomethine nitrogen.[44] The phenolic ν(Ar─OH) stretching vibration of the Schiff base is observed at 1137 cm^{-1},[45] which is shifted by 11–15 cm^{-1} towards lower wavenumbers or disappears in the spectra of the complexes, thus indicating coordination of the phenolic oxygen to the metal ions.[46]

The υ(C═O) band of the ligand at 1655 cm^{-1}, related to the exocyclic carbonyl group, is shifted by 14–25 cm^{-1} to lower energies in the spectra of complexes **1**, **2**, **4**–**6**. This indicates that the exocyclic carbonyl oxygen

10990739, 2019, 11, Downloaded from https://onlinelibrary.wiley.com/doi/10.1002/aoc.5185 by Republic of Moldova Hinari NPL, Wiley Online Library on [18/09/2023]. See the Terms and Conditions (https://onlinelibrary.wiley.com/terms-and-conditions) on Wiley Online Library for rules of use; OA articles are governed by the applicable Creative Commons License

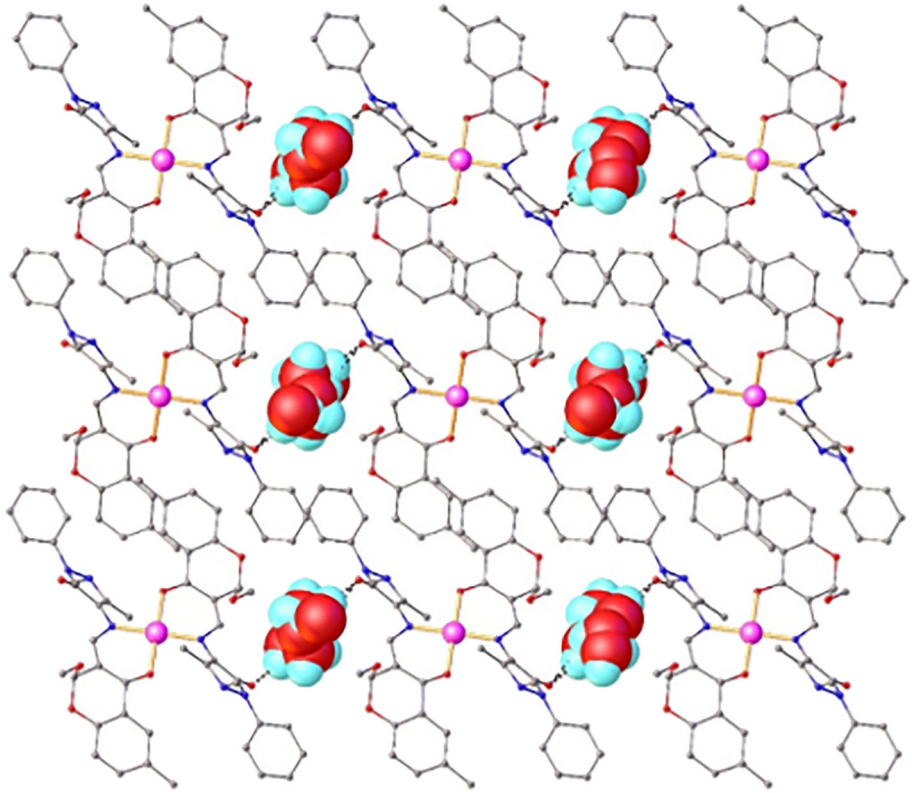


FIGURE 4 View of the crystal structure packing along *b*-axis. Co-crystallized water molecules are shown in space-filling representation

is bonded to the metallic ions.[47] In the IR spectra of complexes **3** and **7**, υ(C═O) band remains unmodified, indicating that the exocyclic ketonic oxygen of the antipyrine ring is not involved in coordination.[48]

In the IR spectra of complexes **1**, **3**, **4** and **6** a considerable peak observed in the range 3450–3420 cm^{-1} supports the presence of υ(H_2O) band.[49]

3.3 | ^{1}H NMR and ^{13}C NMR spectra

The ^{1}H NMR (DMSO-d_6) spectra of diamagnetic Zn(II), Cd(II) and Pt(II) complexes showed the disappearance of the signal due to the OH proton indicating the deprotonation of this group. The signals of the HC═N protons shift downfield in the spectra of the complexes and appeared at 8.40, 8.70 and 8.90 ppm. In the ^{13}C NMR (DMSO-d_6) spectra of the three complexes it was observed that the C═O carbon atom signal shifts downfield and appears at 159.07, 159.13 and 159.24 ppm, respectively. This result indicates the coordination of the metal centre to the azomethine nitrogen, phenolate and keto oxygen atoms.[50]

3.4 | Electronic spectra and magnetic studies

The electronic spectrum of HL in the polycrystalline state shows the intraligand absorption maxima corresponding to $\pi \rightarrow \pi^*$ and $n \rightarrow \pi^*$ transitions: 32 850 and 30 070 cm^{-1}. In the spectra of the complexes these bands are shifted to lower energies (Table 3).

For copper complex **1**, the electronic spectrum (Figure S1) shows an absorption band at 15 030 cm^{-1} which was attributed to the d–d transitions, $^2B_2 \rightarrow {}^2B_1$ and $^2B_2 \rightarrow {}^2A_1$, suggesting a pseudo-tetrahedral geometry for the metal centre. The magnetic moment of the complex (1.78 BM) is normal for Cu(II) with pseudo-tetrahedral stereochemistry.[51]

The electronic spectrum of cobalt complex **2** displayed two bands at 14 200 and 17 500 cm^{-1} assignable to $^4T_{1g}(F) \rightarrow {}^4A_{2g}(F)$ and $^4T_{1g}(F) \rightarrow {}^4T_{1g}(P)$ transitions, respectively, consistent with high-spin octahedral Co(II).[52] The magnetic moment value and the brown colour for this complex are more consistent with octahedral stereochemistry.[53]

The electronic spectra of complexes **3** and **4** showed a square-planar geometry for the Pd and Pt ions. The very

10990739, 2019, 11, Downloaded from https://onlinelibrary.wiley.com/doi/10.1002/aoc.5185 by Republic of Moldova Hinari NPL, Wiley Online Library on [18/09/2023]. See the Terms and Conditions (https://onlinelibrary.wiley.com/terms-and-conditions) on Wiley Online Library for rules of use; OA articles are governed by the applicable Creative Commons License

TABLE 3 Electronic spectral assignments (cm^{-1}) of complexes **1–4**, **7**

Compound	Transitions d–d (cm^{-1})			μ_{eff} (BM)	Geometry
1	$^2B_2 \rightarrow {}^2B_1$, $^2B_2 \rightarrow {}^2A_1$ 15 030			1.78	Pseudo-tetrahedral
2	$^4T_{1g}(F) \rightarrow {}^4T_{2g}(P)$ —	$^4T_{1g}(F) \rightarrow {}^4A_{2g}(F)$ 14 200	$^4T_{1g}(F) \rightarrow {}^4T_{1g}(P)$ 17 500	4.64	Octahedral
3	$^1A_{1g} \rightarrow {}^1B_{1g}$ —	$^1A_{1g} \rightarrow {}^1A_{2g}$ 21 270	$^1A_{1g} \rightarrow {}^1E_g$ —	[a]	Square planar
4	$^1A_{1g} \rightarrow {}^1B_{1g}$ —	$^1A_{1g} \rightarrow {}^1A_{2g}$ 20 830	$^1A_{1g} \rightarrow {}^1E_g$ —	[a]	Square planar
7	$^6A_{1g} \rightarrow {}^4T_{1g}$ 12 000	$^6A_{1g} \rightarrow {}^4A_{1g}$ 21 270	$^6A_{1g} \rightarrow {}^4T_{2g}(D)$ 25 000	5.82	Octahedral

[a]Diamagnetic.

intense bands at about 21 270 and 20 830 cm^{-1}, respectively, are assignable to a combination of metal–ligand charge transfer and d–d bands.[54]

The iron complex **7** is paramagnetic with effective magnetic moment value of 5.82 BM. The electronic spectrum exhibited three bands at 12 000, 21 270 and 25 000 cm^{-1} attributed to the $^6A_{1g} \rightarrow {}^4T_{1g}$, $^6A_{1g} \rightarrow {}^4A_{1g}$ and $^6A_{1g} \rightarrow {}^4T_{2g}(D)$ transitions, respectively, in an octahedral geometry.[44,55]

3.5 | Mass spectra

The FAB mass spectra of complexes **1–7** were recorded (Table S2). The mass spectrum of the ligand showed a peak at $m/z = 429.0$ corresponding to the molecular ion $[M]^+$ (Figure S2). The molecular ion $[M]^+$ peaks obtained from the complexes are as follows: $m/z = 507.4$ (**1**), $m/z = 821.9$ (**2**), $m/z = 868.8$ (**3**), $m/z = 644.9$ (**4**), $m/z = 502.8$ (**5**), $m/z = 574.5$ (**6**), $m/z = 863.9$ (**7**). The data obtained are in good agreement with the proposed molecular formulas for complexes **1–7**. The FAB mass spectra of these complexes show peaks assignable to various fragments arising from the thermal cleavage of the complexes.

3.6 | Thermal decomposition

All the complexes were investigated using thermogravimetric analysis. For compounds **1**, **3**, **4** and **6**, the thermogravimetric analyses show a weight loss in the range 30–120°C. This mass loss corresponds to the elimination of two water molecules for complex **6** and one molecule of water of dehydration for each of complexes **1**, **3** and **4**. In the case of complex **7**, at 160°C there was a weight loss corresponding to two molecules of coordinating water. The second weight loss steps correspond to the release of small coordinated anions: Br^- and Cl^-. The other weight loss corresponds to the decomposition of the ligand. The residue corresponds to the percentage of metal oxide specific to the complexes analysed (Figure S3).

3.7 | Biological activity

3.7.1 | Antibacterial and antifungal activities

The metal complexes **1–7** and the ligand were tested for their *in vitro* antibacterial activity against Gram-positive bacteria (*S. aureus*, *B. cereus*, *E. faecalis*) and Gram-negative bacteria (*E. coli*, *A. baumannii*) and antifungal activity (*C. albicans*, *C. krusei*, *C. neoformans*) using the paper disc diffusion technique (for qualitative determination) and the serial dilutions in liquid broth method (for determination of MIC). Furacillinum, ciprofloxacin, amikacin, nystatin and miconazole were used as standard drugs.

Experimental results obtained from the study of antibacterial activity (Tables 4 and 5) demonstrate that complexes display bacteriostatic and bactericidal activity in the concentration range 0.0019–0.25 mg ml^{-1} towards Gram-positive bacteria and 0.0312–0.5 mg ml^{-1} towards Gram-negative bacteria.

The results of the antimicrobial evaluation revealed that the ligand HL shows good activity against *S. aureus*. It is worth mentioning an increased antibacterial effect in the case of compounds **2** and **5** towards the Gram-positive bacteria *S. aureus*, *B. cereus* and *E. faecalis*. Complexes **2** and **5** showed comparable activity to furacillinum and ciprofloxacin.

The results of antifungal activity (Table 6) of the complexes indicated that among all strains, *C. albicans* and *C. neoformans* were the most susceptible to the compounds. Complex **5** was determined to have MIC value of 0.0312 mg ml^{-1} against *C. albicans* and *C. krusei* while that of nystatine was 0.032 mg ml^{-1}. The iron(III) complex (**7**)

10990739, 2019, 11, Downloaded from https://onlinelibrary.wiley.com/doi/10.1002/aoc.5185 by Republic of Moldova Hinari NPL, Wiley Online Library on [18/09/2023]. See the Terms and Conditions (https://onlinelibrary.wiley.com/terms-and-conditions) on Wiley Online Library for rules of use; OA articles are governed by the applicable Creative Commons License

TABLE 4 Antibacterial activities of ligand HL and complexes as MIC[a]/MBC[b] values (mg ml^{-1})

	Staphylococcus aureus (G+)		*Bacillus cereus* (G+)		*Enterococcus faecalis* (G+)	
Compound	**MIC**	**MBC**	**MIC**	**MBC**	**MIC**	**MBC**
HL	0.0078	0.0156	0.0312	0.0625	0.125	0.25
1	0.0625	0.125	0.0312	0.0625	0.125	0.25
2	0.0039	0.0078	0.0019	0.0039	0.0039	0.0078
3	0.0312	0.0625	0.0156	0.0312	0.125	—
5	0.0019	0.0039	0.0039	0.0078	0.0078	0.0156
6	0.0625	0.125	0.0156	0.0312	0.0312	0.0625
7	0.0625	0.125	0.0312	0.0625	0.125	—
Furacillinum	0.0046	0.0093	0.0046	0.0046	0.037	0.075
Ciprofloxacin	0.001	0.002	0.0003	0.0007	0.0015	0.0031

Staphylococcus aureus (ATCC 25923), *Bacillus cereus* (ATCC 11778), *Enterococcus faecalis* (ATCC 19433). G(+), Gram-positive bacteria.

[a]MIC, minimum inhibitory concentration.

[b]MBC, minimum bactericidal concentration.

TABLE 5 Antibacterial activities of ligand HL and complexes as MIC[a]/MBC[b] values (mg ml^{-1})

	Escherichia coli (G−)		*Acinetobacter baumannii* (G−)	
Compound	**MIC**	**MBC**	**MIC**	**MBC**
HL	0.0312	0.0625	0.25	0.5
1	0.5	—	0.25	0.5
2	0.0625	0.125	0.25	0.5
3	0.125	0.25	0.25	—
5	0.0312	0.0625	0.0312	0.0625
6	0.0625	0.125	0.25	0.5
7	0.0625	0.125	0.125	0.25
Furacillinum	0.0046	0.0046	0.0046	0.0093
Amikacin	0.008	0.016	0.004	0.008

Escherichia coli (ATCC 25922), *Acinetobacter baumannii* (ATCC BAA-747). G(−), Gram-negative bacteria.

[a]MIC, minimum inhibitory concentration.

[b]MBC, minimum bactericidal concentration.

TABLE 6 Antifungal activities of ligand HL and complexes as MIC[a]/MFC[b] values (mg ml^{-1})

	Candida albicans		*Candida krusei*		*Cryptococcus neoformans*	
Compound	**MIC**	**MFC**	**MIC**	**MFC**	**MIC**	**MFC**
HL	0.0625	0.125	0.0312	0.0625	0.0019	0.0039
1	0.25	0.5	0.25	0.5	0.0625	0.125
2	0.0625	0.125	0.0312	0.125	0.0039	0.0078
3	0.125	0.25	0.125	—	0.0039	0.0078
5	0.0312	0.0625	0.0312	0.0625	0.0039	0.0078
6	0.0625	0.125	0.0625	0.25	0.0039	0.0078
7	0.0156	0.0156	0.0625	0.125	0.0078	0.0156
Nystatin	0.032	0.064	0.032	0.064	0.032	0.064
Miconazole	0.016	0.032	0.016	0.032	0.0162	0.032

Candida albicans ATCC 10231, *Candida krusei* ATCC 6258, *Cryptococcus neoformans*

[a]MIC, minimum inhibitory concentration.

[b]MFC, minimum fungicidal concentration.

was the most potent compound of the series, with MIC value of 0.0156 mg ml^{-1} against *C. albicans*. This complex has a better antifungal effect than nystatin and miconazole. The ligand and metal complexes (except for complex **1**) showed good antifungal activity against *C. neoformans* when compared with standard drugs nystatin and miconazole.

3.7.2 | Antiproliferative activity

The results of the reduction rate of Alamar blue indicator used to evaluate the viability of living cells based on their mitochondrial activity have been shown to vary, as follows: Tables S3–S7 present the cell viability of MSC, A375, B16 4A5, HT-29 and MCF-7 cell lines after 24 h exposure to the test substances (1, 2.5, 5, 7.5, 10 μM). Viability is expressed as percentage of viable cells compared to control.

Figure 5 shows the effects of Schiff base HL and complexes **1**–**7** on the viability of the MSC, A375, B16 4A5, HT-29 and MCF-7 cell lines. The final concentrations were 10, 7.5, 5, 2.5 and 1 μM.

The substances did not show any significant antiproliferative activity against MSC cells (Figure 5a), A375 cells

10990739, 2019, 11, Downloaded from https://onlinelibrary.wiley.com/doi/10.1002/aoc.5185 by Republic of Moldova Hinari NPL, Wiley Online Library on [18/09/2023]. See the Terms and Conditions (https://onlinelibrary.wiley.com/terms-and-conditions) on Wiley Online Library for rules of use; OA articles are governed by the applicable Creative Commons License

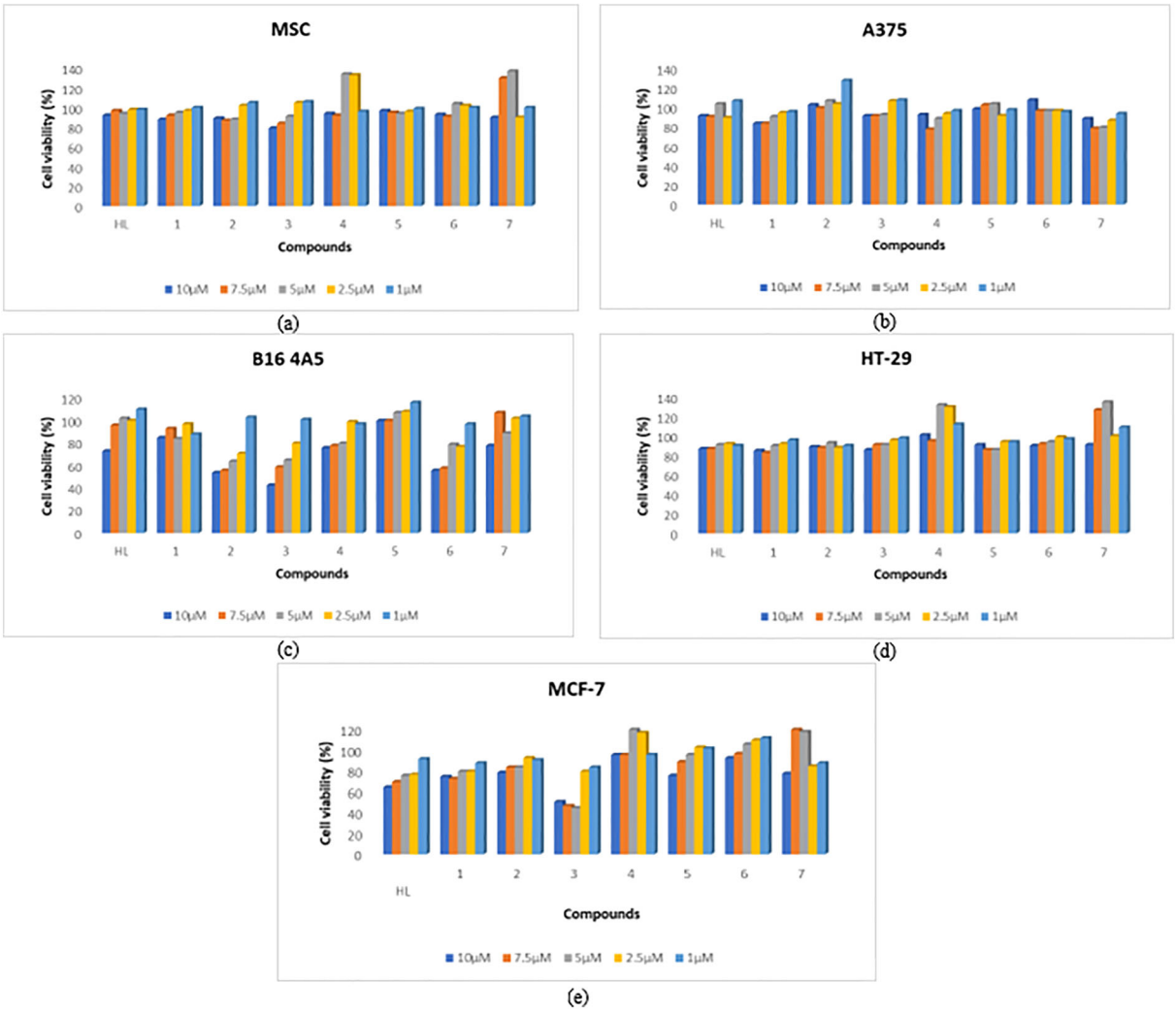


FIGURE 5 Cell viability of the MSC (a), A375 (b), B16 4A5 (c), HT-29 (d) and MCF-7 (e) cell lines after 24 h of treatment with Schiff base HL and its metal complexes **1**–**7**

(Figure 5b) or HT-29 cells (Figure 5d). The inhibition was more than 90% for all tested substances. Therefore no IC_{50} was determined.

Significant *in vitro* antiproliferative activity was found for B16 4A5 cells (Figure 5c). At the highest concentration (10 μM) a significant cytotoxic effect of complexes **2**, **3** and **6** was observed, while at the other concentrations (1, 2.5, 5, 7 μM) there was no evidence of significant antiproliferative activity. Therefore the calculated IC_{50} values for complexes **2**, **3** and **6** against B16 4A5 cells are evident at the concentration of 10 μM. Results are as follows: 54.27 ± 15% for complex **2**, 41.57 ± 0.2% for complex **3**, 52.94 ± 12% for complex **6**. Only a slightly increased cytotoxic activity was observed for the other five substances against B16 4A5 cells.

Complex **3** proved to be active also against MCF-7 cells (Figure 5e). The lowest cell viability (less than 50%) was obtained at the higher concentrations (10, 7.5 and 5 μM). An inhibitory and dose-dependent cytotoxic effect was observed with IC_{50} values of 49.29 ± 7.52% at 10 μM, 45.42 ± 17.31% at 7.5 μM and 43.84 ± 23.04% at 5 μM. The other substances proved to exert only a moderate cytotoxic effect.

The cell lines were analysed also after 48 h exposure to the test substances but without significant decrease of the viability/statistical significance.

The concentration of DMSO used for the preparation of the stock solutions was also evaluated. It was observed that at these concentrations of DMSO (0.1 and 0.2%) there was no significant effect on cell proliferation.

In the case of HEp-2, BxPC-3, MDCK and L20B cell lines, the ligand HL and its metal complexes (Table S8) were tested as inhibitors of cell proliferation using four concentrations: 0.1, 1.0, 10 and 100 μM. The ligand does not exhibit an antiproliferative effect against the Hep-2, BxPC-3, RD and L20B cancer cell lines (Figure 6). Also, it does not inhibit the growth of normal MDCK cells in the concentration range 0.1–100 μM. Complex **5** is active

10990739, 2019, 11, Downloaded from https://onlinelibrary.wiley.com/doi/10.1002/aoc.5185 by Republic of Moldova Hinari NBL, Wiley Online Library on [18/09/2023]. See the Terms and Conditions (https://onlinelibrary.wiley.com/terms-and-conditions) on Wiley Online Library for rules of use; OA articles are governed by the applicable Creative Commons License

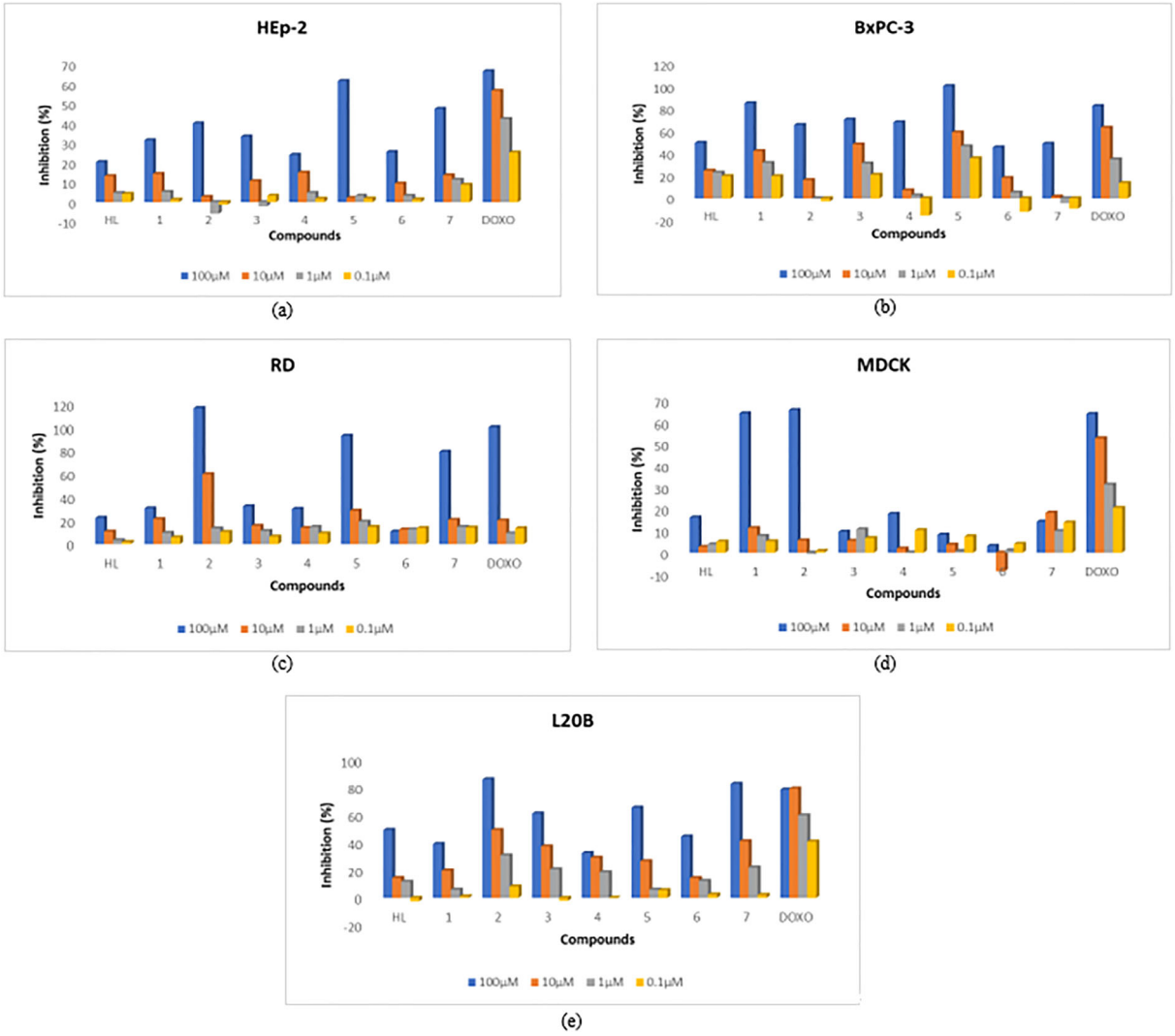


FIGURE 6 Inhibition effect of ligand HL and metal complexes **1–7** against HEp-2 (a), BxPC-3 (b), RD (c), MDCK (d) and L20B (d) cells at four concentrations

against all cancer cell lines studied, where IC_{50} values vary between 1.0 and 77.6 and for BxPC-3 the activity index versus DOX is 3.7 times higher. Complex **6** does not exhibit antiproliferative properties. The antiprolioferative activity of the studied complexes against BxPC-3 cells increases in the following series: Fe(III) < Co(II) < Pt(II) < Pd(II) < Cu(II) < Zn(II). The Fe(III), Zn(II), Pt(II) and Pd(II) complexes do not inhibit the proliferation of normal MDCK cells as opposed to DOX and Cu(II) complex. Complexes **2** and **7** are active against the L20B cell line, where IC_{50} values are 15.4 and 7.4, respectively.

3.8 | Molecular modelling studies

The biological activity of the ligand and the Pd and Zn complexes were analysed computationally by performing molecular docking studies. In virtual screening, the antibacterial activities of the ligand and its Zn complex were tested on *S. aureus* nucleoside diphosphate kinase. Its crystallographic structure is identified by PDB ID: 3Q89.[56] Also, the antiproliferative activities of the ligand and its Pd complex were determined for AKT, a protein kinase which plays a significant role in many processes of the cell like proliferation, apoptosis and glucose metabolism. This is the main reason for taking into account this signalling pathway involvement in proliferation of

TABLE 7 Free binding energies for ligand HL and complexes **3** and **5**

Antibacterial – ID receptor: 3Q89 (kcal mol^{-1})		Antiproliferative – ID receptor: 3L9L (kcal mol^{-1})	
HL	Complex 5	HL	Complex 3
−9.6	−11.0	−5.4	−7.8
−9.3	−10.2	−5.4	−7.5
−9.3	−9.2	−5.3	−7.5

10990739, 2019, 11, Downloaded from https://onlinelibrary.wiley.com/doi/10.1002/aoc.5185 by Republic of Moldova Hinari NPL, Wiley Online Library on [18/09/2023]. See the Terms and Conditions (https://onlinelibrary.wiley.com/terms-and-conditions) on Wiley Online Library for rules of use; OA articles are governed by the applicable Creative Commons License

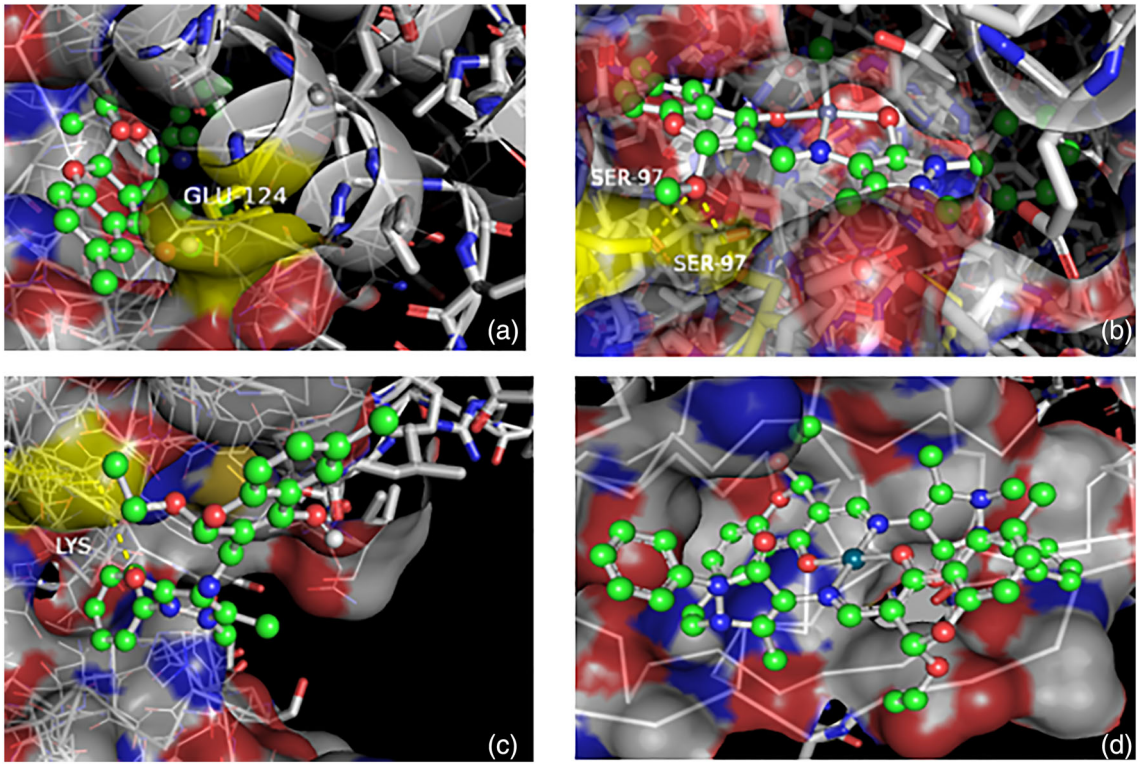


FIGURE 7 Three-dimensional representation of the lowest binding energy interactions of ligand (a) and Zn complex (b) with *Staphylococcus aureus* nucleoside diphosphate kinase and the interaction of ligand (c) and Pd complex (d) with protein kinase

tumour cells. The crystallographic structure has ID PDB: 3L9L.[57] By setting the maximum number of binding modes to three, in Table 7 is presented for each docked compound the values of the free binding energies. It is evident from the results obtained that the presence of metallic ion in molecule decreases the energies but increases the binding affinity. As a consequence, this reveals the superior biological potential of the complexes.

\In Figure 7 are shown the images of the conformations of target proteins with each compound. Yellow dashed lines represent hydrogen bonds. In the interaction with 3Q89, the ligand stabilized a hydrogen bond between the hydrogen from the hydroxyl moiety and oxygen from glutamic acid (Glu124). On the other hand, the Zn complex created a dual hydrogen bonding network composed of oxygen from the methoxy moiety and the two Ser97 (chain A and B). The interaction between the ligand and the protein target in cancer, AKT, is characterized by the formation of a hydrogen bond with Lys189 from the B chain. The interaction between the enzyme and Pd complex is nonpolar because it has no hydrogen bonds.

4 | CONCLUSIONS

The composition and the structure of the newly obtained complexes were confirmed using analytical and physicochemical analyses. In all but one of the complexes, the ligand HL acts in a mononegative tridentate manner around the metal ion, while in complex **3** it acts in a mononegative bidentate manner. The structure of complex **3** has been determined by single-crystal X-ray diffraction, showing that the Pd(II) centre has a square-planar geometry. From the analytical studies, complexes **1**, **5** and **6** have been assigned tetrahedral geometry, while **4** has square-planar geometry and **2** and **7** have octahedral geometry.

The quantitative antimicrobial activity results proved that the ligand and the complexes have specific antimicrobial activity, depending on the microbial species tested and the nature of the metal ion. The Co(II) and Zn(II) complexes have demonstrated a good antibacterial effect against *S. aureus*, *B. cereus* and *E. faecalis*, while the Fe(III) complex has significant antifungal effect against *C. albicans*. Also, the synthesized compounds exhibited good antifungal activity against *C. neoformans* compared to the standard.

Screening for antiproliferative activity of nine cancer cell lines showed a cytotoxic effect of Co(II), Pd(II) and Cd(II) complexes against B16 4A5 murine melanoma cells. The Zn(II) complex is active against HEp-2, RD and MDCK cancer cell lines, where IC_{50} values vary between 1.0 and 77.6 and for BxPC-3 the activity index versus DOX is 3.7 times higher.

The significant binding energies obtained by performing molecular docking would suggest that

10990739, 2019, 11, Downloaded from https://onlinelibrary.wiley.com/doi/10.1002/aoc.5185 by Republic of Moldova Hinari NPL, Wiley Online Library on [18/09/2023]. See the Terms and Conditions (https://onlinelibrary.wiley.com/terms-and-conditions) on Wiley Online Library for rules of use; OA articles are governed by the applicable Creative Commons License

especially the complexes with transitional metals could be more potent biocompounds than the ligand.

We believe that the obtained results add value to our research study in this field and will guide our future studies.

ACKNOWLEDGEMENTS

This study was financially supported by 'Carol Davila' University of Medicine and Pharmacy through contract no. CNFIS-FDI-2019-0534 (MEDEX-II) funded by the Ministry of National Education of Romania, from the Institutional Development Fund for Public Universities – FDI 2019.

ORCID

Elena Pahonțu https://orcid.org/0000-0002-6522-7033
Mihaela Badea https://orcid.org/0000-0002-4018-7610

REFERENCES

[1] W. A. Zoubi, *Int. J. Org. Chem.* **2013**, *3*, 73.

[2] S. Malik, B. Nema, *Int. J. Theor. Appl. Sci.* **2016**, *8*, 28.

[3] R. H. Taha, Z. A. El-Shafiey, A. A. Salman, E. M. El-Fakharany, M. M. Mansour, *J. Mol. Struct.* **2019**, *1181*, 536.

[4] M. Sayed Alam, J. H. Choi, D. U. Lee, *Bioorg. Med. Chem.* **2012**, *20*, 4103.

[5] A. M. Vijesh, A. M. Isloor, P. Shetty, S. Sudarshan, H. K. Fun, *Eur. J. Med. Chem.* **2013**, *62*, 410.

[6] H. Keypour, H. Khanmohammadi, K. P. Wainwright, M. R. Taylor, *Inorg. Chim. Acta* **2004**, *357*, 1283.

[7] G. B. Bagihalli, P. G. Avaji, S. A. Patil, P. S. Badamiet, *Eur. J. Med. Chem.* **2009**, *44*, 2904.

[8] R. B. Bedfort, D. W. Bruce, R. M. Frost, J. W. Goodby, M. Hirdb, *Chem. Commun.* **2004**, *24*, 2822.

[9] K. P. Bryliakov, E. P. Talsi, P. Evgenii, *Angew. Chem. Int. Ed.* **2004**, *43*, 5228.

[10] M. Sedighipoor, A. H. Kianfar, W. A. K. Mahmood, M. H. Azarian, *Polyhedron* **2017**, *129*, 1.

[11] M. C. Godoy, M. R. Fighera, F. R. Souza, A. E. Flores, M. A. Rubin, M. R. Oliveira, N. Zanatta, M. A. P. Martin, H. G. Bonacorso, C. F. Mello, *Eur. J. Pharmacol.* **2004**, *496*, 93.

[12] E. S. H. Ei Ashry, L. F. Awad, E. I. Ibrahim, O. K. Bdeewy, *Chinese J. Chem.* **2007**, *25*, 570.

[13] P. M. P. Santos, A. M. M. Antunes, J. Noronha, E. Fernandes, A. J. S. C. Vieira, *Eur. J. Med. Chem.* **2010**, *45*, 2258.

[14] X. Zhang, *J. Chem. Crystallogr.* **2011**, *41*, 1044.

[15] F. Mahle, T. R. Guimaraes, A. V. Meira, R. Correa, R. C. B. Cruz, A. B. Cruz, R. J. Nunes, V. Cechinel-Filho, F. D. Campos-Buzzi, *Eur. J. Med. Chem.* **2010**, *45*, 4761.

[16] S. Sigroha, B. Narasimhan, P. Kumar, A. Khatkar, K. Ramasamy, V. Mani, M. R. Kumar, A. B. A. Majeed, *Med. Chem. Res.* **2012**, *21*, 3863.

[17] M. Tyagia, S. Chandraa, P. Tyagia, J. Akhtarb, A. Kandanb, B. Singh, *J. Taibah Univ. Sci.* **2017**, *11*, 110.

[18] M. Sayed Alam, D. U. Lee, M. L. Bari, *J. Korean Soc. Appl. Biol. Chem.* **2014**, *57*, 613.

[19] N. Parmar, S. Teraiya, R. Patel, H. Barad, H. Jajda, V. Thakkar, *J. Saudi Chem. Soc.* **2015**, *19*, 36.

[20] D. C. Ilieș, E. Pahonțu, S. Shova, R. Georgescu, N. Stănică, R. Olar, A. Gulea, T. Roșu, *Polyhedron* **2014**, *81*, 123.

[21] P. Kavitha, K. Laxma Reddy, *Arab. J. Chem.* **2016**, *9*, 640.

[22] R. A. Ammar, A. N. M. A. Alaghaz, M. E. Zayed, L. A. Al-Bedair, *J. Mol. Struct.* **2017**, *1141*, 368.

[23] C. Demetgül, N. Beyazit, *Carbohydr. Polym.* **2018**, *1*, 812.

[24] E. S. Jose, J. E. Philip, A. A. Shanty, M. R. P. Kurup, P. V. Mohanan, *Inorg. Chim. Acta* **2018**, *478*, 155.

[25] G. Kalaiarasi, S. Rex Jeya Rajkumar, S. Dharani, N. P. Rath, R. Prabhakaran, *J. Photochem. Photobiol. B.* **2018**, *180*, 77.

[26] A. Barry, Procedures and theoretical considerations for testing antimicrobial agents in agar media, in *Antibiotics in Laboratory Medicine*, 5th ed., Williams and Wilkins, Baltimore, MD **1991** 1.

[27] National Committee for Clinical Laboratory Standard. NCCLS: methods for anti-microbial dilution and disk susceptibility testing of infrequently isolated or fastidious bacteria, Approved guideline. Document M45-A 26(19), NCCLS, Villanova, **1999**.

[28] I. Mantasha, R. Md Kausar, M. Shahid, A. Azaj, A. Musheer, M. K. Ishaat, *Appl. Organometal. Chem.* **2019**, *33*, 1.

[29] M. Naqi Ahamad, M. Shahid, A. Azaj Ansari, M. Kumar, M. K. Ishaat, A. Musheer, Rahisuddin, R. Arif, *New J. Chem.* **2019**, *43*, 7511.

[30] F. Sama, M. Raizada, M. Ashafaq, M. N. Ahamad, I. Mantasha, K. Iman, M. Shahid, Rahisuddin, R. Arif, N. A. Shah, H. A. M. Saleh, *J. Mol. Struct.* **2019**, *1176*, 283.

[31] I. Mantasha, M. Shahid, M. Ahmad, Rahisuddin, R. Arif, S. Tasneem, F. Sama, I. A. Ansari, *New J. Chem.* **2019**, *43*, 622.

[32] D. D. Perrin, W. L. Armarego, D. R. Perrin, *Purification of Laboratory Chemicals*, 2nd ed., Pergamon, New York **1990**.

[33] T. Roșu, E. Pahonțu, C. Maxim, R. Georgescu, N. Stănică, G. L. Almăjan, A. Gulea, *Polyhedron* **2010**, *29*, 757.

[34] J. Fries, H. Getrost, *Organic Reagents for Trace Analysis*, E. Merck, Darmstadt **1977** 291.

[35] CrysAlis RED, *Version 1.171.34.76*, Oxford Diffraction Ltd, Abingdon, UK **2003**.

[36] O. V. Dolomanov, L. J. Bourhis, R. J. Gildea, J. A. K. Howard, H. Puschmann, *J. Appl. Crystallogr.* **2009**, *42*, 339.

[37] G. M. Sheldrick, *Acta Crystallogr.* **2015**, *C71*, 3.

[38] G. M. Morris, R. Huey, W. Lindstrom, M. F. Sanner, R. K. Belew, D. S. Goodsell, A. J. G. Olson, *J. Comput. Chem.* **2009**, *1*, 72.

[39] H. M. Berman, J. Westbrook, Z. Feng, G. Gilliland, T. N. Bhat, H. Weissig, I. N. Shindyalov, P. E. Bourne, *Nucleic Acids Res.* **2000**, *28*, 235.

[40] M. D. Hanwell, D. E. Curtis, D. C. Lonie, T. Vandermeersch, E. Zurek, G. R. Hutchison, *Aust. J. Chem.* **2012**, *4*, 1.

[41] O. Trott, A. J. Olson, *J. Comput. Chem.* **2010**, *31*, 455.

[42] L. Schrödinger, The PyMOL Molecular Graphics System, **2010**.

10990739, 2019, 11, Downloaded from https://onlinelibrary.wiley.com/doi/10.1002/aoc.5185 by Republic of Moldova Hinari NBL, Wiley Online Library on [18/09/2023]. See the Terms and Conditions (https://onlinelibrary.wiley.com/terms-and-conditions) on Wiley Online Library for rules of use; OA articles are governed by the applicable Creative Commons License

[43] W. J. Geary, *Coord. Chem. Rev.* **1971**, *7*, 81.

[44] E. Pahonțu, D. C. Ilieș, S. Shova, C. Oprean, V. Păunescu, O. T. Olaru, F. Ș. Rădulescu, A. Gulea, T. Roșu, D. Drăgănescu, *Molecules* **2017**, *22*, 650.

[45] K. Nakamoto, *Infrared and Raman Spectra of Inorganic and Coordination Compounds*, 5th ed., Wiley-Interscience, New York **1997** 86.

[46] C. Lodeiro, R. Bastida, E. Bertolo, A. Macias, A. Rodriguez, *Polyhedron* **2003**, *22*, 1701.

[47] E. Pahontu, L. I. Socea, S. F. Bărbuceanu, D. C. Ilies, M. Badea, O. T. Olaru, A. Gulea, B. Socea, O. Bratu, *Rev. Chim.* **2018**, *69*, 2959.

[48] B. Sarkar, M. G. B. Drew, M. Estrader, C. Diaz, A. Ghosh, *Polyhedron* **2008**, *27*, 2625.

[49] R. Kannappan, S. Tanase, I. Mutikainen, U. Turpeinen, J. Reedijk, *Polyhedron* **2006**, *25*, 1646.

[50] A. Q. Ali, S. G. Teoh, A. Salhin, N. E. Eltayeb, M. B. K. Ahamed, A. M. S. A. Majid, *Inorg. Chim. Acta* **2014**, *416*, 235.

[51] D. C. Ilieș, S. Shova, V. Rădulescu, E. Pahonțu, T. Roșu, *Polyhedron* **2015**, *97*, 157.

[52] E. Pahonţu, F. Julea, Y. Chumakov, P. Petrenco, T. Roşu, A. Gulea, *J. Organometal. Chem.* **2017**, *836–837*, 44.

[53] T. A. Yousef, O. A. El-Gammal, S. F. Ahmed, G. M. Abu El-Reash, *J. Mol. Struct.* **2014**, *1076*, 227.

[54] D. C. Ilieș, E. Pahonțu, S. Shova, A. Gulea, T. Roșu, *Polyhedron* **2013**, *51*, 307.

[55] E. Pahontu, I. Usataia, V. Graur, Y. Chumakov, P. Petrenko, V. Gudumac, A. Gulea, *Appl. Organometal. Chem.* **2018**, *32*, 1.

[56] S. K. Srivastava, K. Rajasree, B. Gopal, *BBA Proteins Proteomics* **2011**, *1814*, 1349.

[57] Q. Zeng, M. Bourbeau, G. Yao, C. Yuan, S. Zhang, C. Fotsch, C. Dominguez, R. Hungateet, *Bioorg. Med. Chem. Lett.* **2010**, *20*, 1559.

SUPPORTING INFORMATION

Additional supporting information may be found online in the Supporting Information section at the end of the article.

CCDC 1915505 contains the supplementary crystallographic data for this contribution. These data can be obtained free of charge via www.ccdc.cam.ac.uk/conts/retrieving.html (or from the Cambridge Crystallographic Data Centre, 12 Union Road, Cambridge CB2 1EZ, UK; fax: (+44) 1223 336 033; or deposit@ccdc.ca.ac.uk).

How to cite this article: Pahonțu E, Proks M, Shova S, et al. Synthesis, characterization, molecular docking studies and *in vitro* screening of new metal complexes with Schiff base as antimicrobial and antiproliferative agents. *Appl Organometal Chem*. 2019;33:e5185. https://doi.org/10.1002/aoc.5185

10990739, 2019, 11, Downloaded from https://onlinelibrary.wiley.com/doi/10.1002/aoc.5185 by Republic of Moldova Hinari NPL, Wiley Online Library on [18/09/2023]. See the Terms and Conditions (https://onlinelibrary.wiley.com/terms-and-conditions) on Wiley Online Library for rules of use; OA articles are governed by the applicable Creative Commons License